Perspective

Cancer Research

The Relationship between Tumor Blood Flow, Angiogenesis, Tumor Hypoxia, and Aerobic Glycolysis

Leif Østergaard[1,2], Anna Tietze[1,2], Thomas Nielsen[3], Kim Ryun Drasbek[1], Kim Mouridsen[1], Sune Nørhøj Jespersen[1], and Michael R. Horsman[3]

Abstract

Antiangiogenic therapies are being pursued as a means of starving tumors of their energy supply. Although numerous studies show that such therapies render tumors hypoxic, just as many studies have, surprisingly, shown improved tumor oxygenation. These contradicting findings challenge both the original rationale for antiangiogenic therapy and our understanding of the physiology of tissue oxygenation. The flow–diffusion equation, which describes the relation between blood flow and the extraction of freely diffusible molecules in tissue, was recently extended to take the heterogeneity of capillary transit times (CTH) into account. CTH is likely to be high in the chaotic microvasculature of a tumor, increasing the effective shunting of blood through its capillary bed. We review the properties of the extended flow–diffusion equation in tumor tissue. Elevated CTH reduces the extraction of oxygen, glucose, and cytotoxic molecules. The extent to which their net extraction is improved by antiangiogenic therapy, in turn, depends on the extent to which CTH is normalized by the treatment. The extraction of oxygen and glucose are affected to different extents by elevated CTH, and the degree of aerobic glycolysis—known as the Warburg effect—is thus predicted to represent an adaptation to the CTH of the local microvasculature. *Cancer Res; 73(18); 5618–24. ©2013 AACR.*

Introduction

The survival of cancer cells is contingent on their supply of oxygen and nutrients such as glucose via the bloodstream. The establishment and growth of malignant tumors are, therefore, critically dependent on their ability to stimulate the formation of new blood vessels (angiogenesis) to support their metabolic needs (1). During the past few decades, antiangiogenic therapies have been pursued as a means of inhibiting tumor growth (2). Such therapeutic oxygen deprivation might be expected to have unwanted side effects if unsuccessful: Cancer cells become more aggressive, more resistant to chemotherapy and radiation therapy, and more likely to metastasize under hypoxic conditions (3). Surprisingly, antiangiogenic drugs have since been proved to have modest effects on tumor growth when administered alone (4, 5), but to be efficacious in combination with both chemotherapy and irradiation (6, 7)—even beyond an additive effect of the combined treatments (8). These findings have led to the hypothesis that antiangiogenic drugs prune the chaotic tumor microvasculature to provide a more even distribution of blood and anticancer drugs across tumors, thereby improving tissue oxygenation and drug responses (9). In support of this notion, experimental studies have shown that antiangiogenic treatment is followed by a "vascular normalization window," during which microvascular density, length, diameter, and tortuosity are reduced, capillary pericyte coverage is increased, and the basement membrane thickness and capillary permeability to plasma-proteins normalized (7, 10). In some studies, these changes are paralleled by increased tumor oxygenation, and sensitivity to radiation and cytotoxic therapy is significantly increased (7, 10). This is not a consistent finding, however, in that as many studies have shown angiogenesis inhibitors to reduce tumor oxygenation (8, 11).

The finding that reductions in tumor microvascular density can improve tumor oxygenation and the delivery of small molecules to tumor tissue contradicts not only the original rationale for antiangiogenic therapy, but also seems to contradict fundamental principles of physiology and pharmacokinetics. According to these principles, the extraction of diffusible molecules, including oxygen and pharmaceuticals, always decreases if capillary surface area is reduced for a given tumor blood flow (TBF). The cause of this paradox must therefore lie in profound, therapy-related changes either in tumor blood supply or in the extraction of solutes by the tumors.

The blood flow and oxygenation are well characterized in several tumor types (12–15). Most tumors display considerable variability in TBF (mL blood/mL tissue/minute), both within and among tumors of a given type, with TBF ranging from near-zero to several times that of the surrounding, normal tissue

Authors' Affiliations: [1]Center of Functionally Integrative Neuroscience and MIND*Lab*, Department of Clinical Medicine, Aarhus University, Aarhus Denmark; [2]Department of Neuroradiology, and [3]Department of Experimental Clinical Oncology, Aarhus University Hospital, Aarhus, Denmark

Corresponding Author: Leif Østergaard, Center of Functionally Integrative Neuroscience and MIND*Lab*, Department of Neuroradiology, Aarhus University Hospital, Building 10G, 5th Floor, Nørrebrogade 44, DK-8000 Aarhus C, Denmark. Phone: 45-78464091; Fax: 45-78461662; E-mail: leif@cfin.dk

doi: 10.1158/0008-5472.CAN-13-0964

(12, 16). The oxygen extraction fraction (OEF) in tumor tissue is generally poor, ranging from only 5% to 50% of the incoming arterial blood's total oxygen content (12). Most often, blood flow and low oxygen extraction combine to a low availability of oxygen in tumors, as evidenced by oxygen tensions that are generally lower than those of surrounding tissue (12–16). The incomplete extraction of oxygen by tumors with low tissue oxygen tension is characterized as diffusion-limited or chronic hypoxia to indicate that oxygen diffusion from blood tissue must somehow be hindered (16). In some tumors, blood is constantly redistributed across tumor parts (cycling), resulting in what has been dubbed flow limited or acute hypoxia (16).

Chronic hypoxia is traditionally ascribed to increased diffusion distances from capillaries to cells within the chaotic tumor microvasculature, causing cells far from capillaries to receive less oxygen than required (16). This notion is difficult to reconcile with the finding that tumor oxygenation in many cases improves as a result of antiangiogenic treatment, during which average intercapillary distances invariably increase. A more recent hypothesis of chronic tumor hypoxia posits that the microvasculature tends to develop functional arteriovenous shunts in the absence of the normal signaling of metabolic needs among microvessels (17). If vascular normalization restored normal signaling, such shunting might be reduced, the distribution of blood across the microvasculature improved, and oxygen extraction thereby increased (18).

We recently developed a model of the extraction of oxygen and other freely diffusible substances in tissue. The model extends the traditional flow–diffusion equation (19) to take not only blood flow into account, but also the effective shunting that occurs as some blood flows along capillary paths with limited oxygen extraction (see Fig. 1; ref. 20). In this review, we briefly describe the model and then examine its prediction with regards to the net extraction of oxygen, glucose, and cytotoxic molecules under the assumption that tumor angiogenesis is accompanied by increased capillary transit time heterogeneity (CTH). The model predicts that reduced extraction of oxygen, glucose, and cytotoxic molecules is a feature of elevated CTH, and thus of the formation of chaotic tumor vessels. Vascular normalization is predicted to improve tumor oxygenation and the extraction of cytotoxic molecules only when capillary hemodynamics is normalized (CTH reduced) as a result of the antiangiogenic therapy. Meanwhile, therapeutic elevation of TBF is predicted to improve tumor oxygenation only in cases when CTH is moderately elevated. Finally, increased CTH favors the extraction of glucose over oxygen. The degree of aerobic glycolysis—known as the Warburg effect (21)—in tumors is thus predicted to reflect the differential extraction of glucose and oxygen with increasing CTH as a result of tumor angiogenesis.

The relation between TBF and the extraction of diffusible substances: the overlooked importance of CTH

The relation between TBF and the amount of freely diffusible molecules that can be extracted by tumor tissue is derived from the so-called flow–diffusion equation (19). The equation accurately describes the extraction of freely diffusible substances from a single capillary perfused at a given blood

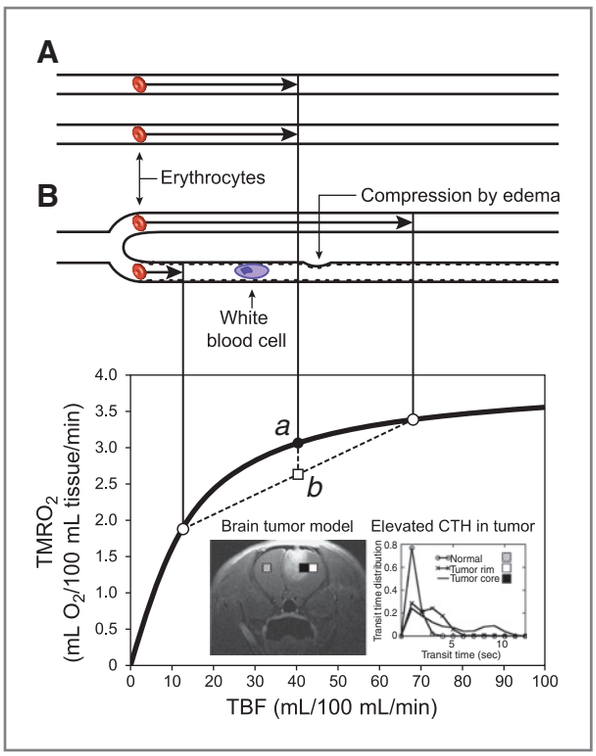

Figure 1. The flow–diffusion relation for oxygen. The classical flow–diffusion equation determines the maximum amount of oxygen that can diffuse from a single capillary into tissue for a given flow velocity. In the graph, flow velocity and oxygen extraction for a single capillary are replaced by tumor blood flow per volume unit (TBF) and net oxygen extraction per tissue volume ($TMRO_2^{max}$) on the *x*- and *y*-axes, respectively. This generalization is only true if all capillary flow velocities are identical. This is most easily understood by observing that net tissue oxygen availability is lower in case B (half of the capillaries have low flows, the other half high flows) than in case A (equal flows), although TBF is identical in the two cases: In the heterogeneous case (B), the net tissue oxygen availability is the average of the oxygen availabilities for the two flows, labeled *b* in the plot. Owing to the concave shape of the TBF–$TMRO_2^{max}$ relation, which holds for capillaries with identical flows, *b* is always smaller than *a*, the oxygen availability for homogenous capillary flows. Sources of poor microcirculatory control across the tumor microvasculature are discussed in detail in ref. 18. Note that several properties of individual tumor capillaries, blood rheology, and tumor microenvironment can hinder a uniform distribution of erythrocytes. These include low-grade inflammation, which increases the adhesion among capillary endothelium and blood cells (indicated by the rugged inner surface of the lower capillary), slow-passing white blood cells, capillary walls with abnormal surface properties and diameters, and capillary compression because of increased interstitial pressure in the tumor. Upstream vasodilation may in fact amplify the redistribution losses shown above, as erythrocytes are forced through other branches at very high speeds, with negligible net oxygenation gains. The image (inset) and the accompanying graph in the lower right of the figure show experimental evidence of the broadening of the distribution of capillary transit time distribution in a 9L rat brain tumor model from work by Quarles and Schmainda (23). Although the distribution of transit times is relatively narrow in normal brain tissue, it is much broadened and CTH thereby elevated in the tumor rim, suggestive of angiogenesis as evidenced by these authors' observations of increased CBV (23). Within the edema/tumor core, the transit time distribution is even broader and CTH more elevated. $TMRO_2^{max}$, maximum tumor metabolic rate of oxygen.

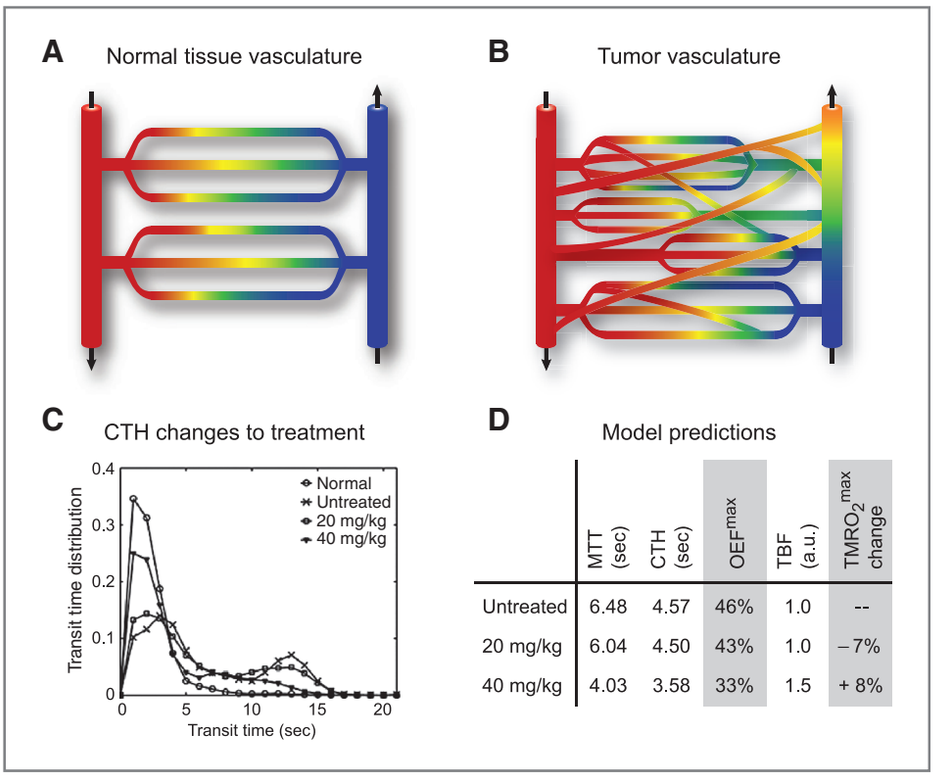

	MTT (sec)	CTH (sec)	OEF^{max}	TBF (a.u.)	$TMRO_2^{max}$ change
Untreated	6.48	4.57	46%	1.0	--
20 mg/kg	6.04	4.50	43%	1.0	−7%
40 mg/kg	4.03	3.58	33%	1.5	+ 8%

Figure 2. Effective shunting of oxygenated blood in capillary networks with heterogeneous, poorly regulated flow velocities. A, illustrates how capillary flow velocities in normal tissue are regulated to provide efficient extraction of oxygen. Red indicates fully oxygenated blood whereas the transition over orange and yellow to blue indicates gradual deoxygenation. In tumors (B), tight control of capillary flow distributions is invariably lost owing to factors such as the lack of normal, contractile pericytes on capillaries, irregular luminal capillary diameters, capillary compression by tumor edema, increased blood cell adhesion to the endothelium, and loss of the conducted vasomotor responses that ensure appropriate blood distribution in normal microvessels (18). The oxygenation response to the removal of specific capillary paths by antiangiogenic therapy in this example depends critically on the resulting redistribution of capillary flows and changes in TBF—estimated here by the CTH and MTT parameters. C, shows the effects of two different doses of an antiangiogenic agent, SU11657, on the distribution of transit times as recorded by Quarles and Schmainda (23). Note how the highest dose almost normalizes distribution of transit times compared to that of normal brain tissue. According to Fig. 1, this homogenization would be expected to improve tumor oxygenation. The first two columns of D show MTT and CTH derived from the pre- and posttreatment transit time distributions in C. As transit time distributions were experimentally determined in this case, we determined the OEF^{max} values shown in the third column using equation one in ref. 20, rather than assuming a gamma variate distribution. We assumed identical tissue oxygen tensions (P_tO_2) of 7.5 mm Hg for all 3 conditions. Note that in this tumor type, treatment with SU11657 caused hemodynamic vascular normalization in the sense that CTH was reduced in a dose-dependent manner. The parallel reductions in MTT, which were the result of reductions in CBV and increased TBF, however, resulted in a predicted reduction in OEF^{max}. The net oxygenation, $TMRO_2^{max}$, is given as the arterial oxygen concentration multiplied by TBF and OEF^{max}. Note that tumor oxygenation increased in the high-dose condition as a net effect of an increase in TBF (23) that outweighed the reduction in OEF^{max}, but decreased in the low-dose experiment. The example underscores the importance of knowing the treatment-related changes in MTT and CTH to predict how the availability of oxygen in a given tumor is affected by various doses of antiangiogenic therapy. a.u., arbitrary units; OEF^{max}, maximum achievable OEF; $TMRO_2^{max}$, maximum tumor metabolic rate of oxygen.

velocity. Replacing capillary flow velocity by tissue blood flow, this equation is now widely used to model the net extraction of freely diffusible substance in tissue, given the net capillary surface area per-unit tissue volume, and their permeability to the substance (19). Figure 1 shows why this generalization from single capillaries to tissue is a gross oversimplification. According to the experimentally proven single-capillary version of the flow–diffusion equation, any degree of capillary flow heterogeneity in tissue is bound to reduce the availability of a diffusible substance in tissue relative to the predictions of the universally applied "tissue version" of this fundamental equation (22). Tumor vessels are highly tortuous and display profound changes in capillary wall morphology and blood cell adhesion (12). Such vascular changes, and possibly increases in local interstitial pressure, have been shown to disturb the distribution of capillary transit times in the tumor tissue. The image insets are reproduced from elegant experiments conducted by Quarles and Schmainda and show elevated transit time heterogeneity in a brain tumor model (23). As shown in Fig. 2B, angiogenesis tends to lower the efficacy of oxygen extraction by effectively shunting oxygenated blood through the tumor microcirculation. Similarly, the oxygenation response to the removal of some of the capillary paths shown in Fig. 2B by antiangiogenic therapy is inherently difficult to predict. Later, we describe a general framework for estimating tumor oxygenation based on capillary transit time patterns such as those shown in Fig. 2C and show how treatment-related changes in capillary transit time patterns can be used to predict parallel changes in the net oxygenation of individual tumors (cf. Fig. 2D).

An extended flow–diffusion equation

We recently extended the flow–diffusion equation to take the effects of CTH into account. The model is described in detail elsewhere (20) and summarized only briefly here. The model assumes a gamma variate distribution of capillary transit times in tissue (24), permitting us to characterize regional tumor hemodynamics by two parameters: the mean transit time (MTT) of blood through the capillaries, and CTH, which for the gamma variate equals the standard deviation of capillary transit times. The MTT is related to TBF and capillary blood volume (CBV, mL blood/mL tissue) through the central volume theorem, MTT = CBV/TBF (25). The maximum achievable extraction fraction (EF^{max}) for a diffusible substance with bidirectional clearance constant k (in sec^{-1}) and a given tissue concentration of the substances can then be determined by integrating over all transit times of the respective capillaries. By doing so, the original flow–diffusion equation is only applied to ensembles of capillaries with identical transit times, thereby avoiding the heterogeneity bias shown in Fig. 1. The resulting EF^{max} for a given diffusible substance now depends on TBF, CBV, CTH, the capillary permeability k of the substance, and its tissue concentration.

Hemodynamic limitations to the extraction fractions of oxygen, glucose, and diffusible molecules in tumors

Figure 3A shows a contour plot of the maximum extraction fractions for oxygen (OEF^{max}) as a function of the MTT and CTH using the hemodynamics of a xenografted human breast carcinoma as an example. The model was calibrated to the metabolic rates and TBF values reported by Kallinowski and colleagues (26; see figure legend). Note that increases in CTH reduce the tumor's ability to extract oxygen for a given tissue oxygen tension. This effect is caused by the increased proportion of blood that passes through the microvasculature too fast to permit proper extraction of diffusible substances as CTH increases for a fixed TBF. CTH reduces the effective capillary surface area available for diffusion for any diffusible substance (including pharmaceuticals) according to the expression $PS = -TBF \ln(1 - EF^{max})$, where PS denotes the effective capillary permeability–surface area product for the substance and EF^{max} is determined by the extended flow–diffusion equation (20).

The tumor's microcirculation is highly chaotic, owing to the aberrant topology, morphology, and patency of newly formed microvessels, the increased vascular permeability and pressure from surrounding fluids and tissue cells, and altered blood rheology (12). Tumor angiogenesis is therefore expected to increase CTH, as shown by the inset in Fig. 1 and indicated by the arrows in Fig. 3A. As indicated by the vertical components of the arrows in Fig. 3A, an increase in CTH caused by angiogenesis can result in a significant reduction in OEF^{max} for a given TBF and tissue oxygen tension. This is consistent with the general finding of lower OEFs in tumors than in their host tissue (12). Also note that TBF is shown to be a poor predictor of tumor oxygenation without simultaneous knowledge of CTH. By definition, angiogenesis increases the CBV. Meanwhile, the tumor expands, and the net CBV per unit of tumor volume may therefore increase, decrease, or remain constant. Note, however, that unless TBF increases in proportion to CBV, then MTT (equal to CBV/TBF), increases. The two cases of either reduced or prolonged MTT are indicated by the horizontal components of the two arrows in Fig. 3A.

The net extraction of diffusible molecules

The upper limit imposed by the tumor's microcirculation on the local metabolic rate of glucose, $TMRglc^{max}$, and oxygen, $TMRO_2^{max}$, can now be determined by multiplying their EF^{max} values by TBF and the arterial concentrations of glucose and oxygen, respectively. Figure 3B shows a surprising feature of high CTH: As indicated by the red arrow, increased TBF, without a concomitant reduction in CTH, can lead to a hemodynamic state (value of MTT and CTH) in which the availability of oxygen is unaltered or even reduced in comparison to the initial hemodynamic state. We refer to this critical level of shunting as malignant CTH and note that it is specific to the diffusion properties of the molecule and its tissue concentration (20). Figure 3B thereby encapsulates the requirements for angiogenesis to subserve the supply of nutrients to a tumor. Although the formation of new vessels is clearly necessary to maintain sufficient vascularization (high CBV) and blood flow (TBF) in a given tissue volume, the chaotic nature of newly tumor vessels (and thus the high CTH) is a crucial limitation to the net amount of nutrients that can be extracted from the new vasculature.

The model predicts that strategies to improve tumor oxygenation by increasing TBF may prove unsuccessful unless the tumor's microcirculation permits CTH to decrease in response to the increased flow rate (see the oblique arrow in Fig. 3B). Similarly, the model predicts that antiangiogenic treatment can improve tumor oxygenation, and the extraction of cytotoxic molecules, by reducing CTH. Although CTH has been shown to decrease in response to one antiangiogenic agent (cf. Fig. 2C and 2D), the schematic drawing in Fig. 2B illustrates that tumor oxygenation responses are likely to depend critically on the way in which the microvascular "pruning" affects the shunting of oxygenated blood. As illustrated by Fig. 2D, this uncertainty may explain the variability of tumor oxygenation changes after antiangiogenic therapy (8, 11) and may suggest measurements of CTH and MTT responses to antiangiogenic therapy across tumors as a means of understanding these oxygenation responses.

Aerobic glycolysis

The iso-contour plot in Fig. 3C shows the net oxygen:glucose extraction ratio (OGR). Oxidative phosphorylation of glucose (complete breakdown of glucose to ATP) requires oxygen to be present in a ratio of approximately 5–6:1, whereas a relative lack of oxygen will result in the conversion of some glucose into lactate instead—glycolysis. Note that the differential extraction of glucose and oxygen results in a close dependency of OGR upon MTT and CTH. The anticipated changes in tumor hemodynamics as a result of angiogenesis (cf. inset in Fig. 1) thus imply that tissue will have relatively easier access to glucose than to oxygen in tumors with a more chaotic microcirculation. The term "aerobic glycolysis" was originally coined

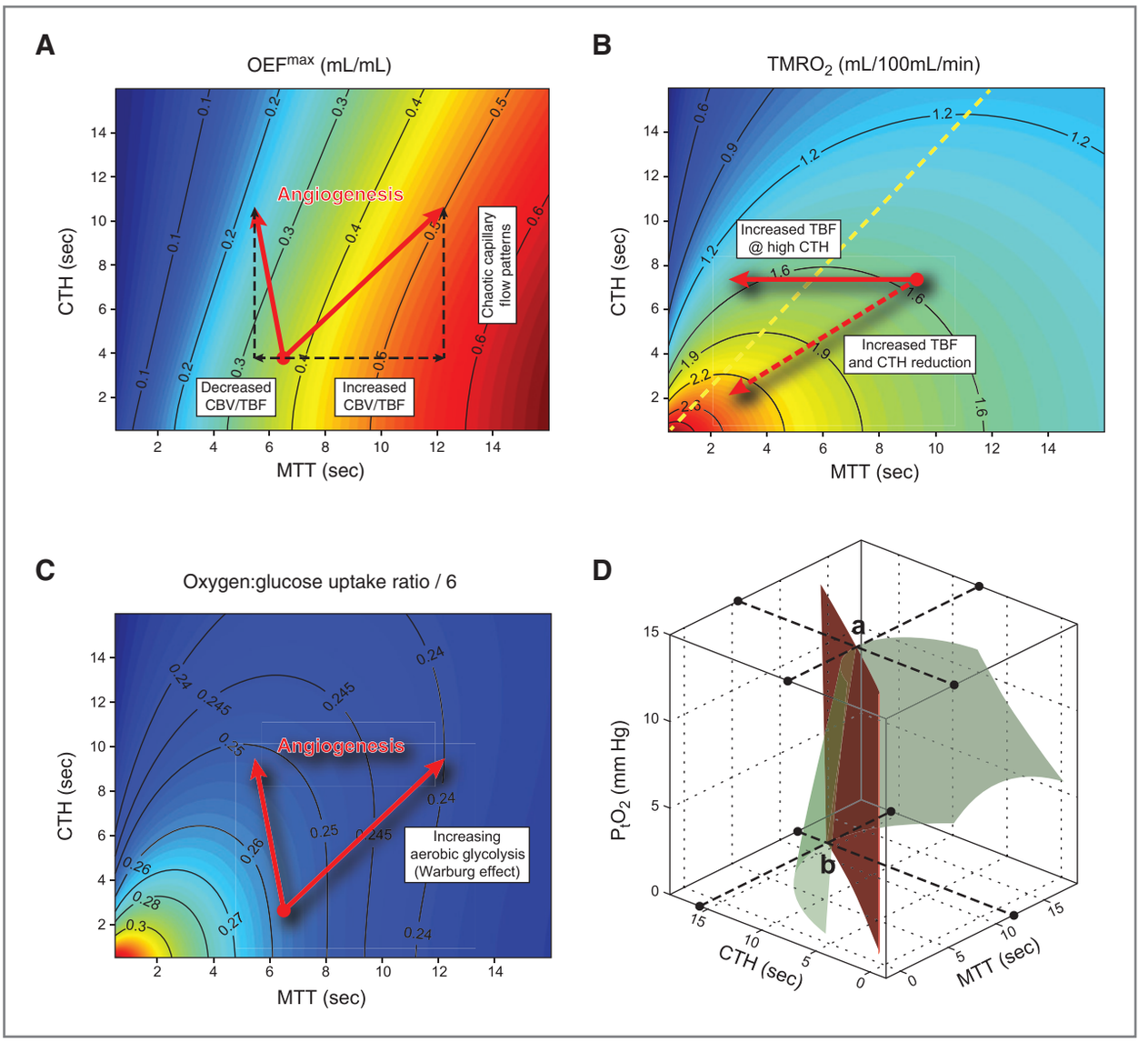

Figure 3. The relation between MTT, CTH, tumor oxygen tension, and the extraction efficacy and net availability of oxygen and glucose in tumors. A and B show model predictions of OEF^{max} and $TMRO_2{}^{max}$ in a tumor model for which TBF and resting metabolism values were available for model calibration (see Table 1 in ref. 26). We chose xenografted breast carcinoma grown to a size of around 2.5 g (35 ± 1 days) in mice, for which TBF = 16 mL/100 mL/min, $TMRO_2$ = 1.18 mL/100 mL/min, OEF = 0.46. To calibrate the model parameter *k* for oxygen, we assumed P_tO_2 to be 7.5 mm Hg, and set CBV to 3 mL/100 mL (corresponding to MTT = 11.25 seconds) and CTH to 95% of MTT under these conditions. The arterial blood oxygen concentration was set to 0.185 mL/mL. The OEF^{max} value that corresponds to a given location in the (MTT, CTH) plane is best inferred from the OEF^{max} values indicated on the two nearest solid OEF^{max} iso-contours. Note that increases in CTH always reduce OEF^{max} for fixed MTT (or TBF) and tissue oxygen tension. Note that for combinations of MTT and CTH above the yellow dashed line in B, incremental increases in TBF (reductions in MTT) no longer improve tumor oxygenation. As shown by the arrows, the improvement of tumor oxygenation by elevating TBF is contingent on the simultaneous homogenization of capillary flows to reduce the effective shunting of blood at high CTH values. We calculated the corresponding values for glucose, assuming TMRglc = 43 μmol/100 g/min and measured extraction fraction of glucose (EFglc) = 0.34 (see Table 1 in ref. 26). We assumed the tissue concentrations of glucose to be 1.25 mmol/L, and an arterial glucose concentration of 7.76 mmol/L. C shows $TMRO_2{}^{max}$/6 $TMRglc^{max}$. When this ratio is unity, the vasculature can support glucose utilization by oxidative phosphorylation. Note how both elevated MTT (low TBF) and elevated CTH owing to tumor angiogenesis, tends to necessitate ATP generation by aerobic glycolysis. The green surface in D corresponds to combinations of MTT, CTH, and P_tO_2, for which oxygen availability precisely matches the $TMRO_2$ of the xenografted breast carcinoma in B ($TMRO_2$ = 1.18 mL/100 mL/min; ref. 26). The interior of the half-cone therefore represents combinations of MTT, CTH, and P_tO_2 for which this the metabolic needs of this tumor type can be met. The red plane marks the boundary of malignant CTH, to the left of which increased TBF would reduce tumor oxygenation. Note that as CTH increases, for example at a tissue P_tO_2 of 15 mm Hg, tumor oxygen metabolism can no longer be supported as CTH reaches the critical limit indicated by *a*. The model predicts that as CTH increases further, the metabolic needs of the tumor can only be met provided TBF can be suppressed (MTT prolonged) and P_tO_2 reduced. The resulting decrease in the degree of shunting and improved blood–tissue concentration gradient permit higher levels of CTH, until oxygenation finally becomes critical as P_tO_2 approaches 0. OEF^{max}, maximum achievable OEF; TMRglc, measured tumor metabolic rate of glucose; $TMRO_2$, measured tumor metabolic rate of oxygen; $TMRO_2{}^{max}$, maximum tumor metabolic rate of oxygen.

by Otto Warburg (21), who detected the phenomenon in tumor cells *in vitro*. This phenomenon, and its relation to other cancer traits (27), could in theory reflect cellular adaptations to the prevalent nutrients permitted by the tumor's microcirculation.

Poor oxygen extraction from a chaotic tumor microcirculation: the role of tumor hypoxia

The elevated CTH of tumor vasculature reduces the extraction of oxygen for a fixed tissue oxygen tension (cf. Fig. 3A). The tumor's oxidative metabolism constantly metabolizes oxygen, and as the extraction of oxygen becomes limited by elevated CTH, this consumption therefore tends to reduce tissue oxygen tension. Consequently, blood–tissue oxygen concentration gradient—and thereby OEF^{max}—increases. Figure 3D illustrates how tumor hypoxia permits the tumor to cover its oxygen needs, even if CTH continues to increase during angiogenesis. The green surface corresponds to combinations of MTT, CTH, and tumor oxygen tension, for which oxygen availability precisely matches the MRO_2 of the xenografted breast carcinoma used for illustration in Fig. 3A–C ($TMRO_2$ = 1.18 mL/100 mL/min, according to ref. 26). The bell-shaped interior of the surface therefore represents combinations of MTT, CTH, and tumor oxygen tension for which the metabolic needs of this tumor type can be met. The red plane marks the boundary of malignant CTH, to the left of which increased TBF would reduce tissue oxygen availability. The label *a* shows the theoretical maximum for the increase in CTH (indicated by a broken line parallel to the MTT axis) that can be sustained by tumor tissue at a tissue oxygen tension (P_tO_2) level of 15 mm Hg. Assuming for a moment that CTH increases while CBV (the CBV per tissue volume) remains constant during tumor angiogenesis, then CTH ultimately reaches a critical limit (label *b*), where oxygen tension cannot be reduced further. At this time, the tumor effectively outgrows its vasculature, and necrosis is predicted to ensue. Note that MTT increases by a factor of two as CTH increases between condition *a* and *b*, i.e., TBF is reduced by a factor of two. As CTH increases for a fixed CBV, the metabolic needs of the tumor can therefore be met by reducing TBF to ensure a higher oxygen extraction. This is consistent with the general finding of lower TBF in tumors than in their host tissue (12).

Discussion

The tendency of the tumor microcirculation to lose normal hemodynamic control has been described and modeled in detail by Pries and colleagues (17, 18), who also coined the associated "shunt problem": poor extraction of oxygen, glucose, and pharmaceuticals in tumors as blood is effectively shunted through capillaries with poorly controlled flow (18). The extent to which the extraction of diffusible substances is reduced by the loss of normal hemodynamic control across the capillary bed can be addressed by advanced simulation models of the microcirculation (17, 18). The extended flow–diffusion model (20), in its current form, does not account for nonuniform substance concentrations and spatial diffusion properties at the microscopic level (see discussion in ref. 20). By these simplifications, it permits us to address salient features of the shunt problem for oxygen, glucose, and freely diffusible pharmaceuticals, based on tumor MTT (or blood flow) and CTH. Both these parameters can be derived from the retention of intravascular contrast agents in the tumor vasculature as observed by dynamic MRI, computerized tomography, or contrast-enhanced ultrasound (23, 28–30), as exemplified in Figs. 1 (inset) and 2C. In principle, these techniques can therefore be applied in human malignancies in relation to therapies that target the tumor microvasculture. In preclinical models, intravital optical imaging techniques (10) provide an additional means to achieve this information.

We propose that MTT and CTH estimates may predict the oxygenation status of tumors, their metabolic status in terms of ATP yields from mixed oxidative phosphorylation and glycolysis (27), and their uptake of freely diffusible molecules. Our analysis of MTT and CTH data obtained in an experimental tumor model shows that CTH can be normalized in part by antiangiogenic therapy (23) but further suggests that the change in tumor oxygenation depends on parallel changes in MTT (cf. Fig. 2D). Although these findings reemphasize the need to understand tumor angiogenesis and hemodynamic control (17, 18), they also suggest that existing diagnostic imaging techniques can be used to identify hemodynamic impairments of tumor oxygenation in relation to individualized cancer therapy.

Disclosure of Potential Conflicts of Interest

No potential conflicts of interest were disclosed.

Authors' Contributions

Conception and design: L. Østergaard
Development of methodology: L. Østergaard, K. Mouridsen, S.N. Jespersen
Analysis and interpretation of data (e.g., statistical analysis, biostatistics, computational analysis): L. Østergaard, S.N. Jespersen
Writing, review, and/or revision of the manuscript: L. Østergaard, A. Tietze, T. Nielsen, K.R. Drasbek, K. Mouridsen, Michael R Horsman
Administrative, technical, or material support (i.e., reporting or organizing data, constructing databases): L. Østergaard, S.N. Jespersen
Study supervision: L. Østergaard

Acknowledgments

This work was supported by the Danish National Research Foundation (CFIN; L. Østergaard, K. Mouridsen, S.N. Jespersen), the Danish Ministry for Research, Innovation, and Education (MIND*Lab*; L. Østergaard, A. Tietze, K.R. Drasbek, K. Mouridsen, S.N. Jespersen), and the Lundbeck Foundation (CIRRO, T. Nielsen)

Received April 2, 2013; revised May 30, 2013; accepted June 1, 2013; published OnlineFirst June 13, 2013.

References

1. Ferrara N. VEGF and the quest for tumour angiogenesis factors. Nat Rev Cancer 2002;2:795–803.
2. Folkman J. Tumor angiogenesis: therapeutic implications. N Engl J Med 1971;285:1182–6.

3. Hockel M, Vaupel P. Tumor hypoxia: definitions and current clinical, biologic, and molecular aspects. J Natl Cancer Inst 2001;93:266–76.
4. Yang JC, Haworth L, Sherry RM, Hwu P, Schwartzentruber DJ, Topalian SL, et al. A randomized trial of bevacizumab, an anti-vascular endothelial growth factor antibody, for metastatic renal cancer. N Engl J Med 2003;349:427–34.
5. Cobleigh MA, Langmuir VK, Sledge GW, Miller KD, Haney L, Novotny WF, et al. A phase I/II dose-escalation trial of bevacizumab in previously treated metastatic breast cancer. Semin Oncol 2003;30(5 Suppl 16):117–24.
6. Hurwitz H, Fehrenbacher L, Novotny W, Cartwright T, Hainsworth J, Heim W, et al. Bevacizumab plus irinotecan, fluorouracil, and leucovorin for metastatic colorectal cancer. N Engl J Med 2004;350:2335–42.
7. Goel S, Duda DG, Xu L, Munn LL, Boucher Y, Fukumura D, et al. Normalization of the vasculature for treatment of cancer and other diseases. Physiol Rev 2011;91:1071–121.
8. Horsman MR, Siemann DW. Pathophysiologic effects of vascular-targeting agents and the implications for combination with conventional therapies. Cancer Res 2006;66:11520–39.
9. Jain RK. Normalization of tumor vasculature: an emerging concept in antiangiogenic therapy. Science 2005;307:58–62.
10. Fukumura D, Duda DG, Munn LL, Jain RK. Tumor microvasculature and microenvironment: novel insights through intravital imaging in preclinical models. Microcirculation 2010;17:206–25.
11. Siemann DW, Dai Y, Horsman MR. Hypoxia, metastasis, and anti-angiogenic therapies In: Melilli G, editor. Hypoxia and cancer: biological implications and therapeutic opportunities. New York: Springer; 2013.
12. Vaupel P, Kallinowski F, Okunieff P. Blood flow, oxygen and nutrient supply, and metabolic microenvironment of human tumors: a review. Cancer Res 1989;49:6449–65.
13. Vaupel P, Hockel M, Mayer A. Detection and characterization of tumor hypoxia using pO_2 histography. Antioxid Redox Signal 2007; 9:1221–35.
14. Vaupel P, Hoeckel M, Mayer A. Oxygenation status of urogenital tumors. Adv Exp Med Biol 2011;701:101–6.
15. Vaupel P, Kelleher DK. Blood flow and oxygenation status of gastrointestinal tumors. Adv Exp Med Biol 2012;737:133–8.
16. Vaupel P. Tumor microenvironmental physiology and its implications for radiation oncology. Semin Radiat Oncol 2004;14:198–206.
17. Pries AR, Cornelissen AJ, Sloot AA, Hinkeldey M, Dreher MR, Hopfner M, et al. Structural adaptation and heterogeneity of normal and tumor microvascular networks. PLoS Comput Biol 2009;5:e1000394.
18. Pries AR, Hopfner M, le Noble F, Dewhirst MW, Secomb TW. The shunt problem: control of functional shunting in normal and tumour vasculature. Nat Rev Cancer 2010;10:587–93.
19. Renkin EM. B. W. zweifach award lecture. regulation of the microcirculation. Microvasc Res 1985;30:251–63.
20. Jespersen SN, Østergaard L. The roles of cerebral blood flow, capillary transit time heterogeneity and oxygen tension in brain oxygenation and metabolism. J Cereb Blood Flow Metab 2012;32:264–77.
21. Warburg O, Posener K, Negelin E. Über den stoffwechsel der tumoren. Biochem Z 1924;152:319–44.
22. Østergaard L, Sorensen AG, Chesler DA, Weisskoff RM, Koroshetz WJ, Wu O, et al. Combined diffusion-weighted and perfusion-weighted flow heterogeneity magnetic resonance imaging in acute stroke. Stroke 2000;31:1097–103.
23. Quarles CC, Schmainda KM. Assessment of the morphological and functional effects of the anti-angiogenic agent SU11657 on 9L gliosarcoma vasculature using dynamic susceptibility contrast MRI. Magn Reson Med 2007;57:680–7.
24. King RB, Raymond GM, Bassingthwaighte JB. Modeling blood flow heterogeneity. Ann Biomed Eng 1996;24:352–72.
25. Stewart GN. Researches on the circulation time in organs and on the influences which affect it. Parts I-III. J Physiol 1894;15:1–89.
26. Kallinowski F, Schlenger KH, Runkel S, Kloes M, Stohrer M, Okunieff P, et al. Blood flow, metabolism, cellular microenvironment, and growth rate of human tumor xenografts. Cancer Res 1989;49:3759–64.
27. Hanahan D, Weinberg RA. Hallmarks of cancer: the next generation. Cell 2011;144:646–74.
28. Østergaard L, Chesler DA, Weisskoff RM, Sorensen AG, Rosen BR. Modeling cerebral blood flow and flow heterogeneity from magnetic resonance residue data. J Cereb Blood Flow Metab 1999;19:690–9.
29. Østergaard L. Principles of cerebral perfusion imaging by bolus tracking. J Magn Reson Imaging 2005;22:710–7.
30. Mouridsen K, Østergaard L, Christensen S, Jespersen SN. Reliable estimation of capillary transit time distributions at voxel level using DSC MRI. In: Proceedings of the International Society of Magnetic Resonance in Medicine; 2011 May 7–13; Montréal, Canada. International Society of Magnetic Resonance in Medicine; 2011. p 3915.